ACS Chemical Neuroscience

Research Article

pubs.acs.org/chemneuro

Quantum Dot Conjugates of GABA and Muscimol: Binding to $\alpha1\beta2\gamma2$ and $\rho1$ $GABA_A$ Receptors

Hélène A. Gussin,[†] Ian D. Tomlinson,[‡] Dingcai Cao,[†] Haohua Qian,[†,∥] Sandra J. Rosenthal,[‡,§] and David R. Pepperberg*[,†]

[†]Lions of Illinois Eye Research Institute, Department of Ophthalmology and Visual Sciences, University of Illinois at Chicago, Chicago, Illinois 60612, United States

[‡]Department of Chemistry and [§]Departments of Physics, Chemical & Biomolecular Engineering, and Pharmacology, Vanderbilt University, Nashville, Tennessee 37235, United States

[∥]National Eye Institute, National Institutes of Health, Bethesda, Maryland 20892, United States

ABSTRACT: $GABA_A$ receptors are ligand-gated ion channels that mediate inhibitory synaptic signaling in the CNS. Fluorescent probes with the ability to target these receptors can provide insights into receptor location, distribution and dynamics in live cells, while revealing abnormalities in their distribution and dynamics that could occur in a variety of diseases. We have developed fluorescent probes of $GABA_A$ receptors that are composed of a CdSe/ZnS core−shell nanocrystal (quantum dot; qdot) conjugated to pegylated derivatives of the GABA receptor agonists GABA and muscimol (GABA-qdots and muscimol-qdots, respectively). Quantitative fluorescence imaging was used to analyze the binding activity of these conjugates to $\alpha1\beta2\gamma2$ $GABA_A$ and $\rho1$ $GABA_A$ receptors expressed in *Xenopus* oocytes. The selectivity of these conjugates for $\alpha1\beta2\gamma2$ $GABA_A$ and $\rho1$ $GABA_A$ receptors was determined by their ability to compete with the antagonists bicuculline and methyl-(1,2,3,6-tetrahydropyridin-4-yl)phosphinic acid (TPMPA). Both GABA- and muscimol-qdots exhibited robust binding to both $\alpha1\beta2\gamma2$ and $\rho1$ $GABA_A$ receptors. At $\alpha1\beta2\gamma2$ receptors, pretreatment with bicuculline reduced conjugate binding by ≥8-fold on average, an extent far exceeding the reduction produced by TPMPA (∼30%). Conversely, at $\rho1$ receptors, pretreatment with TPMPA inhibited binding by ∼10-fold, an extent greatly exceeding the change produced by bicuculline (∼50% or less). These results indicate specific binding of muscimol-qdots and GABA-qdots to $\alpha1\beta2\gamma2$ $GABA_A$ and $\rho1$ $GABA_A$ receptors in a manner that preserves the respective pharmacological sensitivities of these receptors to TPMPA and bicuculline, and encourage the use of qdot-conjugated neurotransmitter analogs as labeling agents at $GABA_A$ receptors.

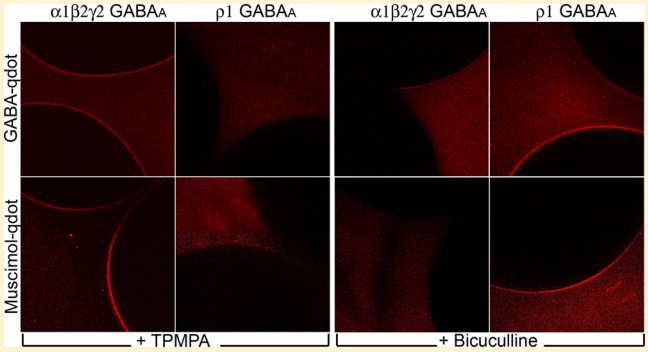

KEYWORDS: *GABA receptor, ligand-gated ion channel, muscimol, GABA, quantum dot conjugate, nanocrystal*

γ-Aminobutyric acid (GABA) is a major inhibitory neurotransmitter of the central nervous system. $GABA_A$ receptors, a class of ligand-gated ion channels, represent a major subtype of GABA receptors, and are important pharmacological targets for benzodiazepines, barbiturates, and anesthetics. Their structure is a pentameric arrangement of α, β, γ, δ, ε, π, and/or θ subunits.[1−4] $GABA_A$-ρ (also known as $GABA_C$) receptors are a subfamily of $GABA_A$ receptors that consist of ρ subunits.[3,5−12] $GABA_A$-non-ρ and $GABA_A$-ρ receptors exhibit distinct pharmacological properties. For example, while GABA and muscimol (5-aminomethyl-3-hydroxyisoxazole) are agonists of both $GABA_A$-non-ρ and $GABA_A$-ρ receptors, bicuculline is an antagonist of $GABA_A$-non-ρ receptors only, and (1,2,5,6-tetrahydropyridin-4-yl)methylphosphinic acid (TPMPA) and 2-aminoethyl methylphosphonate are antagonists of $GABA_A$-ρ receptors.[13−17]

Quantum-dot-conjugated, chain-derivatized analogues of GABA receptor agonists[18] are potentially useful for fluorescence labeling of GABA receptors, allowing, for example, the study of location, distribution, and membrane dynamics of GABA receptors in live cell cultures. Cadmium selenide−zinc sulfide (CdSe/ZnS) core−shell nanocrystals, or quantum dots (qdots), are highly fluorescent semiconductor crystals with quantum yields approaching unity.[19] Their photostability allows continuous excitation for periods of hours, rather than minutes or seconds as currently achievable with organic fluorescent dyes. The emission spectra of core−shell nanocrystals are narrow and size-tunable, enabling their application in multiplex imaging studies.[20−23] Thus, qdot conjugates of biomolecules are an emerging alternative to dye conjugates in applications that require long acquisition times or high detection sensitivity.

Received: August 31, 2012
Accepted: December 5, 2012
Published: December 5, 2012

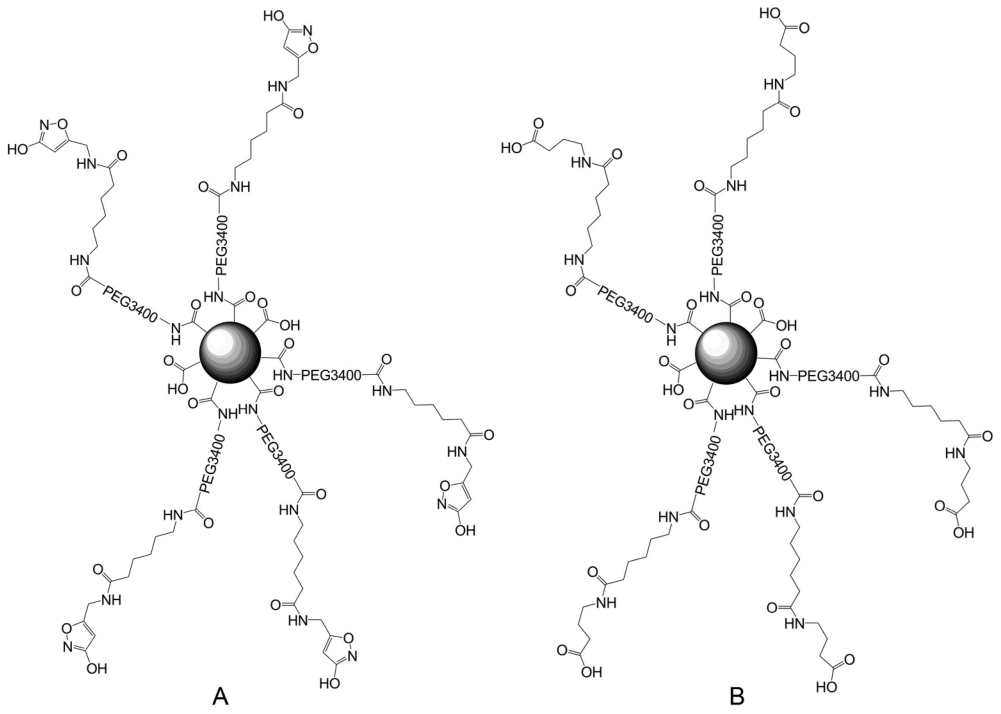

Figure 1. Schematic representation of muscimol-conjugated (A) and GABA-conjugated (B) quantum dot. Panel A reproduced with permission from ref 40. Copyright 2006 American Chemical Society.

To date, qdots have been conjugated to a variety of biomolecules, through acid−base interactions between the ligand and the surface of the qdot,[24] covalent attachment of the ligand to a polymer coating on the qdot,[25] or interactions between a biotinylated ligand and a streptavidin coat on the qdot.[26−39] Among the previously described types of qdot-based constructs that have been used to study membrane bound receptors are those consisting of small-molecule ligands conjugated to the qdot via a linear linker. For example, Gussin et al.[40] and Tomlinson et al.[41] have shown, by quantitative image analysis, that muscimol linked to highly fluorescent, AMP-coated CdSe/ZnS quantum dots via an aminohexanoyl spacer and a poly(ethylene glycol) chain (muscimol-qdot; ∼150−200 copies of muscimol/qdot; Figure 1A) exhibits specific binding to *Xenopus* oocytes expressing ρ1 $GABA_A$ receptors, a homopentameric model of $GABA_A$-ρ receptors.[5,11,42−45] Furthermore, the binding intensity is correlated with the number of muscimol-terminated chains joined to the qdot.[46]

The high multivalency (e.g., number of muscimols bound to a given qdot; Figure 1A) and other features of the previously described muscimol-qdot raise interesting questions about the nature of the binding interaction of this type of molecule with GABA receptors. In the present study, we have further investigated this interaction by determining whether muscimol-qdots (Figure 1A) and a closely related conjugate that incorporates GABA as the terminating ligand (Figure 1B) exhibit binding to $\alpha1\beta2\gamma2$ $GABA_A$ receptors, a widely distributed $GABA_A$ receptor subtype. Specifically, we have asked whether interactions of the qdot-based conjugates with $\alpha1\beta2\gamma2$ $GABA_A$ and ρ1 $GABA_A$ receptors preserve the selective sensitivity of these receptor subtypes to bicuculline and TPMPA antagonists. The results provide evidence for robust binding of muscimol- and GABA-qdots to $\alpha1\beta2\gamma2$ $GABA_A$ as well as ρ1 $GABA_A$ receptors, and indicate marked subtype-dependent inhibition of the conjugate/receptor interaction. Preliminary findings were reported at the 2009 meeting of the Society for Neuroscience.[47]

RESULTS AND DISCUSSION

Synthesis of Ligand-Conjugated Quantum Dots. We synthesized a GABA-derivatized ligand, which was conjugated to the AMP-qdot polymer surface. Briefly, this ligand was composed of GABA derivatized with an aminohexanoyl linker that was subsequently attached to an amino-terminated polydisperse poly(ethylene glycol) (PEG) chain with an average mass of 3400 Da. This ligand was conjugated to the AMP surface of the qdot using EDC coupling as previously described.[40] This yielded GABA-conjugated qdots that contained ∼150−200 GABA ligands attached to the qdot (Figure 1B). Preparation of the muscimol-qdot conjugate followed previously described procedures.[40]

Binding of Conjugates to GABA Receptor-Expressing Oocytes. To test for specific binding of the GABA-conjugated qdots (GABA-qdots) and muscimol-conjugated qdots (muscimol-qdots) to $GABA_A$ receptors, we incubated the conjugates, at approximately 30 nM (qdot concentration), with oocytes expressing either $\alpha1\beta2\gamma2$ or homopentameric ρ1 $GABA_A$ receptors, or with nonexpressing (NE) oocytes. Incubation of $\alpha1\beta2\gamma2$-expressing and ρ1-expressing oocytes with either muscimol-qdots or GABA-qdots yielded a fluorescent halo at the oocyte surface membrane, indicating binding of the qdot-conjugate to the oocyte surface. This halo was absent following similar treatment of NE oocytes (Figure 2). Net halo fluorescence intensity (FI), that is, halo intensity minus surround background intensity,[40,46] was significantly higher in $\alpha1\beta2\gamma2$- or ρ1-expressing oocytes than in NE oocytes, with either muscimol-qdots [FI($\alpha1\beta2\gamma2$) vs FI(NE): 51.53 (mean) ± 21.66 (SD) (n = 9) vs 10.74 ± 9.62 (n = 10), p < 0.0001; FI(ρ1) vs FI(NE): 65.81 ± 14.43 (n = 8) vs 10.74 ± 9.62 (n =

dx.doi.org/10.1021/cn300144v | ACS Chem. Neurosci. 2013, 4, 435−443

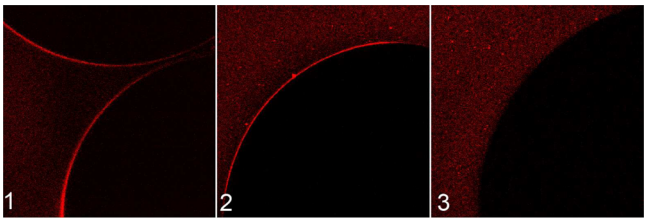

Figure 2. Fluorescence images of oocytes following 15 min incubation with 30 nM GABA-qdots. Oocytes expressed either $\alpha1\beta2\gamma2$ (panel 1) or $\rho1$ (panel 2) $GABA_A$ receptors, or were nonexpressing controls (panel 3). (Note the presence of two oocytes in the panel 1 image.) Similar results were obtained using a muscimol-qdot conjugate (data not shown).

10), $p < 0.0001$] or GABA-qdots [FI($\alpha1\beta2\gamma2$) vs FI(NE): 37.35 ± 21.03 ($n = 6$) vs 7.20 ± 15.15 ($n = 9$), $p = 0.0032$; FI ($\rho1$) vs FI(NE): 47.78 ± 26.54 ($n = 9$) vs 7.20 ± 15.15 ($n = 9$), $p = 0.0005$].

Figure 3 illustrates the development of fluorescence intensity over time. At all time points the net fluorescence obtained with

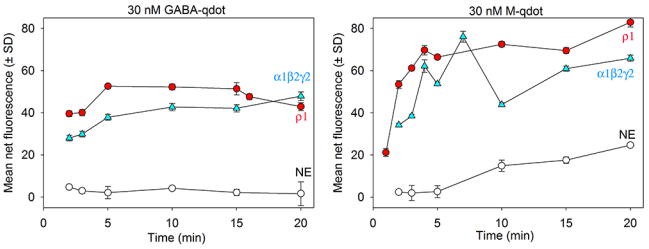

Figure 3. Net fluorescence intensities determined for $\alpha1\beta2\gamma2$- (blue) and $\rho1$- (red) $GABA_A$ receptor expressing oocytes, and for nonexpressing oocytes (open circles), upon incubation with 30 nM GABA-qdots or muscimol-qdots. For each data point, net fluorescence intensity was obtained by normalizing the mean fluorescence based upon the mean of the background. Incubation periods ranged from 2 to 20 min.

nonexpressing oocytes was relatively low, whereas the fluorescence obtained with both qdot conjugates on GABA receptor-expressing oocytes was significantly higher than background. Average FI values obtained with a given GABA receptor subtype were slightly higher for muscimol-qdots than for GABA-qdots. As the potencies of free muscimol and GABA at the two receptor types are comparable,[48−50] this modest difference may have reflected differing orientations of the two terminating ligands in the receptor's GABA-binding pocket due to chain-derivatization. The relative plateaus evident in the graphs are consistent with previous reports, which showed that ∼80% of the maximal fluorescence intensity was reached after a 5 min incubation.[40,46]

Competition, by Free Muscimol or Free GABA, of Conjugate Binding to GABA Receptor-Expressing Oocytes. In competition experiments, we asked whether preincubation of oocytes with free muscimol or GABA decreases binding of the qdot conjugate. To assess competition by free ligand, we first incubated the oocytes for 15 min with free GABA or free muscimol at a fixed concentration (500 μM), and then with a solution containing both the same free ligand (500 μM) and a given qdot conjugate (30 nM). We first consider the results obtained with the use of GABA-qdots and free GABA as competitor. The two panels at the upper left of Figure 4 show representative images obtained with $\alpha1\beta2\gamma2$-

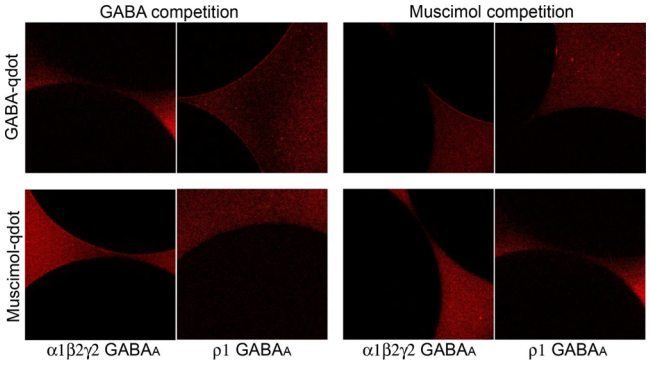

Figure 4. Fluorescence images of oocytes following 15 min incubation with 30 nM GABA-qdots (top row) or muscimol-qdots (bottom row), supplemented with 500 μM free GABA (left) or 500 μM free muscimol (right). Oocytes expressed either $\alpha1\beta2\gamma2$ or $\rho1$ $GABA_A$ receptors, as indicated.

and $\rho1$-expressing oocytes when the duration of the incubation with coapplied GABA-qdots and GABA was 15 min. Fluorescence intensities determined under this experimental condition were significantly lower than those determined in experiments that involved only a 15 min incubation with 30 nM GABA-qdots alone [$\alpha1\beta2\gamma2$: 0.47 ± 0.66 ($n = 2$) vs 37.35 ± 21.03 ($n = 6$), $p = 0.0284$; $\rho1$: 6.84 ± 5.35 ($n = 4$) vs 47.78 ± 26.54 ($n = 9$), $p = 0.0062$]. Similar results were obtained with muscimol-qdots (representative images shown in Figure 4, lower left). That is, FI values obtained with added GABA were significantly lower than those obtained with muscimol-qdots alone [$\alpha1\beta2\gamma2$: 4.78 ± 4.79 ($n = 6$) vs 51.53 ± 21.66 ($n = 9$), $p = 0.0001$; $\rho1$: 2.74 ± 3.32 ($n = 4$) vs 65.81 ± 14.43 ($n = 8$), $p < 0.0001$]. Competition with muscimol yielded a similar pattern of results for both GABA-qdots and muscimol-qdots (Figure 4, upper and lower right). These results, which are consistent with those previously reported,[40] indicated that under all of the investigated conditions, competition with free ligand markedly decreased the fluorescence halo.

Figure 5 shows mean net fluorescence intensities of the halo when GABA-qdot and muscimol-qdot conjugates were competed with free GABA or free muscimol for binding to oocytes expressing $\alpha1\beta2\gamma2$ (left) or $\rho1$ receptors (right). The

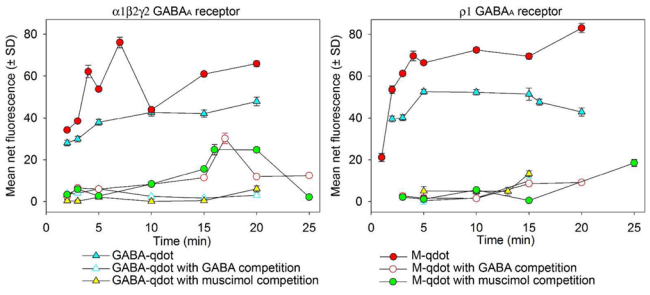

Figure 5. Mean net fluorescence intensity of the halo when GABA-qdot and muscimol-qdot conjugates were competed with free GABA or free muscimol for binding to oocytes expressing $\alpha1\beta2\gamma2$- (left) and $\rho1$- (right) $GABA_A$ receptors. Data were obtained on incubation of the oocytes with GABA and qdot conjugate (GABA-qdots, open blue triangles; muscimol-qdots, open red circles); or on incubation with muscimol and qdot conjugate (GABA-qdots, yellow triangles; muscimol-qdots, green circles). For comparison, Figure 3 results obtained in the absence of competitor are also shown (filled blue and filled red symbols for GABA-qdots and muscimol-qdots, respectively).

dx.doi.org/10.1021/cn300144v | ACS Chem. Neurosci. 2013, 4, 435−443

values obtained when the oocytes were incubated with GABA and the qdot conjugate (open blue and red symbols) are relatively low (i.e., mean FI not different from background), by contrast with the values obtained in the absence of competitor (filled blue and red symbols). The effect of added competitor on mean net fluorescence intensity after a fixed period of treatment can be represented as the FI value determined under a given condition (i.e., given qdot conjugate and receptor type) with added competitor normalized to that determined under the same condition in the absence of competitor. Table 1

Table 1. Effect of Test Agents on the Binding of Qdot Conjugates[a]

		oocyte-expressed $GABA_A$ receptor	
row	treatment	$\alpha1\beta2\gamma2$	$\rho1$
1	GABA-qdot	1	1
2	GABA-qdot + muscimol	**0.00 ± 0.00** (p = 0.027)	**0.25 ± 0.33** (p = 0.015)
3	GABA-qdot + GABA	**0.01 ± 0.02** (p = 0.028)	**0.14 ± 0.14** (p = 0.006)
4	GABA-qdot + TPMPA	0.74 ± 0.42 (p = 0.28)	**0.08 ± 0.14** (p < 0.001)
5	GABA-qdot + bicuculline	**0.12 ± 0.24** (p = 0.010)	1.07 ± 1.14 (p = 0.59)
6	muscimol-qdot	1	1
7	muscimol-qdot + muscimol	**0.07 ± 0.11** (p < 0.001)	**0.01 ± 0.02** (p < 0.001)
8	muscimol-qdot + GABA	**0.09 ± 0.10** (p < 0.001)	**0.04 ± 0.05** (p < 0.001)
9	muscimol-qdot + TPMPA	0.69 ± 0.42 (p = 0.14)	**0.10 ± 0.15** (p < 0.001)
10	muscimol-qdot + bicuculline	**0.03 ± 0.05** (p < 0.001)	0.54 ± 0.14 (p = 0.001)

[a]Results obtained at t = 15 min in experiments of the types described in Figures 4 and 5. Each entry describes FI results obtained with 30 nM qdot conjugate plus 500 μM test agent, upon normalization to results obtained with the qdot conjugate only (mean ± SD); the associated p-value is shown in parentheses. Bold entries denote results for which both the average normalized fluorescence was ≤0.25 and the associated p-value was <0.03, signifying a marked suppression of fluorescence.

reports the normalized results obtained when the period of incubation with coapplied qdots and competitor was 15 min. For example, for both GABA-qdots and muscimol-qdots, when FI values obtained at t =15 min for $\alpha1\beta2\gamma2$- and $\rho1$-expressing oocytes in the presence of free GABA were normalized to FI values obtained under similar conditions but in the absence of GABA, the average ratio was 0.01−0.14 (Table 1, lines 3 and 8). That is, the presence of GABA greatly reduced the FI. When the oocytes were incubated with GABA-qdot and muscimol-qdot conjugates with competition with free muscimol (yellow and green symbols), FI values obtained at t = 15 min were also close to zero. Specifically, with GABA-qdots, FI values obtained with muscimol competition were 0.00 ± 0.00 (n = 2) and 12.23 ± 14.15 (n = 4) for oocytes expressing $\alpha1\beta2\gamma2$ and $\rho1$ receptors, respectively. With muscimol-qdots, muscimol competition yielded FI values of 3.70 ± 5.23 (n = 6) and 0.78 ± 1.11 (n = 2) for oocytes expressing $\alpha1\beta2\gamma2$ and $\rho1$ receptors, respectively. Normalization of the data obtained at t = 15 min with muscimol competition showed that fluorescence in the presence of muscimol was, on average, 0−0.25 of the FI value obtained in the absence of competitor (Table 1, lines 2 and 7). From these results, we conclude that free GABA and free muscimol inhibit the binding of GABA-qdots and muscimol-qdots to $\alpha1\beta2\gamma2$- and $\rho1$-expressing oocytes.

Competition of Muscimol-qdot or GABA-qdot Binding with Bicuculline or TPMPA. In experiments similar in design to that used for the tests of GABA and muscimol as competitors, oocytes expressing $\alpha1\beta2\gamma2$ or $\rho1$ $GABA_A$ receptors were incubated with GABA-qdots or muscimol-qdots, together with methyl-(1,2,3,6-tetrahydropyridin-4-yl)-phosphinic acid (TPMPA), a $GABA_A$ ρ-subtype receptor antagonist, or with bicuculline ($GABA_A$ non-ρ receptor antagonist).[7,13−17] Fluorescence images presented in panels A−D of Figure 6 show results obtained with TPMPA

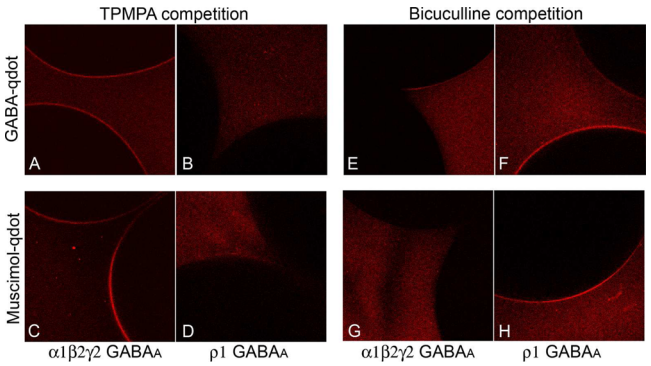

Figure 6. Fluorescence images of oocytes following 15 min incubation with 30 nM GABA-qdots (panels A, B, E, and F) or muscimol-qdots (panels C, D, G, and H) supplemented with the GABA receptor antagonists TPMPA (left) or bicuculline (right). Oocytes expressed either $\alpha1\beta2\gamma2$ (panels A−D) or $\rho1$ (panels E−H) $GABA_A$ receptors, as indicated.

competition. As illustrated in Figure 6, A and C, TPMPA coapplied with GABA-qdots (A) and muscimol-qdots (C) to oocytes expressing $\alpha1\beta2\gamma2$ $GABA_A$ receptors preserved a visually substantial fluorescence halo, but markedly reduced the fluorescence halo at oocytes expressing $\rho1$ $GABA_A$ receptors (B and D). Conversely, for both qdot preparations, bicuculline (Figure 6E−H) essentially eliminated the fluorescence halo at $\alpha1\beta2\gamma2$-expressing oocytes (E and G), but had relatively little effect at $\rho1$-expressing oocytes (F and H). These visual observations were confirmed when fluorescence intensity of the halos was quantified. As shown in the left panel of Figure 7, the binding of GABA-qdots and muscimol-qdots to $\alpha1\beta2\gamma2$ receptors was inhibited by bicuculline (yellow and green symbols). Analysis of fluorescence intensities at $\alpha1\beta2\gamma2$ oocytes, determined in the presence of bicuculline, at t = 15 min yielded 4.35 ± 8.70 (n = 4) and 1.73 ± 2.33 (n = 4) for GABA-qdots and muscimol-qdots, respectively; these were significantly lower than FIs obtained in the absence of competitor (p = 0.0095 for GABA qdots; and p = 0.0005 for muscimol qdots). Furthermore, the effects of TPMPA (open blue and red symbols) on the binding of GABA qdots and muscimol qdots at $\alpha1\beta2\gamma2$ were modest, with FI = 27.55 ± 1.39 (n = 2) and 35.65 ± 15.39 (n = 3), respectively, at t = 15 min; these values did not differ significantly from values at t = 15 min obtained in the absence of competitor (p = 0.2775 for GABA-qdots and p = 0.1318 for muscimol-qdots) (filled blue and red symbols). By contrast, as shown in the right panel of Figure 7, the binding of GABA-qdots and muscimol-qdots to

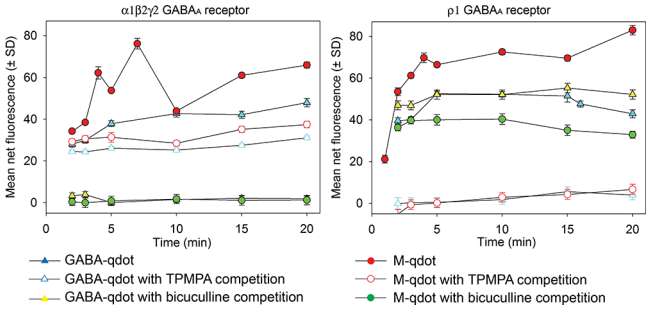

Figure 7. Mean values of net fluorescence intensity of the halo when GABA-qdot and muscimol-qdot conjugates were competed with TPMPA and bicuculline for binding to oocytes expressing $\alpha1\beta2\gamma2$- (left) and $\rho1$- (right) $GABA_A$ receptors. Data were obtained on incubation of the oocytes with TPMPA and qdot conjugate (GABA-qdots, open blue triangles; or muscimol-qdots, open red circles); or on incubation with bicuculline and qdot conjugate (GABA-qdots, yellow triangles; or muscimol-qdots, green circles). For comparison, Figure 3 results obtained in the absence of competitor (filled blue and filled red symbols for GABA-qdots and muscimol-qdots, respectively) are replicated here.

$\rho1$ receptors was inhibited by TPMPA (open blue and red symbols) [at t = 15 min, FI = 4.07 ± 6.46 (n = 6) for GABA-qdots and FI = 6.76 ± 9.61 (n = 6) for muscimol-qdots; p = 0.0009 and p < 0.0001, respectively, when compared to FIs obtained in the absence of competitor], but not by bicuculline (yellow and green symbols) [at t = 15 min, FI = 52.11 ± 46.68 (n = 5) for GABA-qdots (not significantly different from FIs obtained in the absence of competitor; p = 0.413) and FI = 35.23 ± 5.23 (n = 4) for muscimol-qdots (p = 0.0013)]. For $\alpha1\beta2\gamma2$-expressing oocytes, FI values determined in the presence of bicuculline were, on average, 0.12 and 0.03 of those determined with only GABA-qdots and muscimol-qdots, respectively (Table 1, lines 5 and 10). For oocytes expressing $\alpha1\beta2\gamma2$ receptors, FI values in the presence of TPMPA were not as dramatically reduced (Table 1, lines 4 and 9), indicating that bicuculline, but not TPMPA, essentially abolished the binding of the qdot conjugates to $\alpha1\beta2\gamma2$ receptors. When the FI values of $\rho1$-expressing oocytes incubated with bicuculline were normalized to those obtained without bicuculline, the ratios were >1 and 0.54 for GABA-qdots and muscimol-qdots, respectively (Table 1, lines 5 and 10), indicating the absence of a strong effect on binding of the qdot conjugates. By contrast, normalization of FI values obtained in $\rho1$-expressing oocytes in the presence of TPMPA yielded average values of 0.08 for GABA-qdots (line 4) and 0.10 for muscimol-qdots (line 9), indicating that the presence of TPMPA greatly decreased binding of the conjugates to $\rho1$ receptors. Thus, the presence of bicuculline inhibited the binding to $\alpha1\beta2\gamma2$ $GABA_A$ receptors only, while the presence of TPMPA inhibited the binding to $\rho1$ $GABA_A$ receptors only.

Summary and Future Studies. The present study builds on previous work[40,41,46] by examining binding of the muscimol-qdot preparation at non-ρ $GABA_A$ receptors, and investigating the pharmacological specificity of receptor binding by both qdot conjugates. The results demonstrate the binding of both muscimol-qdots and GABA-qdots to both $\alpha1\beta2\gamma2$ $GABA_A$ and $\rho1$ $GABA_A$ receptors expressed in *Xenopus* oocytes. This binding is specific, that is, receptor-dependent, since no binding by either conjugate to nonexpressing oocytes was observed. Furthermore, the specificity of the investigated conjugates for $GABA_A$ non-ρ and $GABA_A$ ρ-subtype receptors is pharmacologically significant. That is, in both receptor types, free GABA and free muscimol compete with binding of both conjugates. In addition, the binding of both conjugates to $\alpha1\beta2\gamma2$ $GABA_A$ receptors is inhibited by bicuculline, an antagonist of $GABA_A$ non-ρ receptors, and binding of both to $\rho1$ $GABA_A$ receptors is inhibited by TPMPA, a $GABA_A$ ρ-subtype receptor antagonist.

The robust and selective binding activity of the qdot conjugates investigated here suggests a number of future applications for these structures. One such application is their use in tracking the movement of single $GABA_A$ receptors on cell surfaces.[51] As emphasized in previous studies, the high fluorescence and nonbleaching nature of these structures offer distinct advantages by comparison with organic fluorophores.[19−23] Furthermore, these conjugates may prove valuable as an alternative to immunolabeling for identifying the locations of $GABA_A$ receptors in neural tissue. A further potential application is one in which qdot-attached linear chains terminated with a reagent other than GABA or muscimol are substituted for some of the GABA- or muscimol-terminated chains, to yield a qdot-based scaffold that can be customized for specific applications. For example, a qdot conjugate possessing biotin-terminated as well as GABA- or muscimol-terminated chains could perhaps function as a scaffold that enables the trapping of single, isolated $GABA_A$-expressing cells on a streptavidin-coated surface for cell biological or physiological study.

A broad question of interest raised by the present findings is the dependence of $GABA_A$ receptor binding affinity and on/off kinetics of the investigated qdot conjugates on structural features such as ligand valency and the length/composition of the linker that joins these ligands to the qdot. The present procedures for obtaining quantitative FI data can be applied generally to determining binding parameters, including the effects of competitors and other pharmacological agents. However, the precise determination and mechanistic interpretation of binding parameters will likely require improvement in the precision with which the absolute number of ligands bound to the qdot (i.e., qdot valency) can be controlled. That is, at present, the maximal number of ligand-terminated chains bound to a given qdot appears to vary from ∼150 to ∼200.[40,46] In addition, because $GABA_A$ receptors possess multiple GABA-binding sites (two on $\alpha1\beta2\gamma2$; five on $\rho1$), kinetic models derived in such studies will need to consider the contributions of multiple binding modes to the interaction of the multivalent conjugate with a given receptor. Also important will be testing of the possibility that a given copy of the conjugate "bridges" neighboring receptors on the cell surface.[46] The addressing of these issues will likely prove valuable for widening the application of qdot-based multivalent conjugates to the targeting of cell surface receptor proteins.

METHODS

Chemical Materials. AMP-coated CdSe/ZnS core−shell qdots (peak emission wavelength λ_{max} = 605 nm) were obtained from Invitrogen by Life Technologies (Carlsbad, CA) and supplied as an 8 μM solution in borate buffer. The AMP polymer coating increased the diameter of the core−shell qdot from approximately 11 nm to about 12−14 nm. *tert*-Butyloxycarbonyl (BOC) amine-poly(ethylene glycol)-*N*-hydroxysuccinimide ester (BOC-NHPEG-NHS; purity >85%) was obtained from Nektar Therapeutics (Huntsville, AL). The poly(ethylene glycol) (PEG) chains of this product had a molecular weight (determined by MALDI) of 3446 Da (approximately 78 ethylene glycol units) and a polydispersity of 1.00. Trifluoroacetic acid (TFA), *N*-hydroxysuccinimide (NHS), 1-[3-(dimethylamino)propyl]-3-ethyl-

dx.doi.org/10.1021/cn300144v | ACS Chem. Neurosci. 2013, 4, 435−443

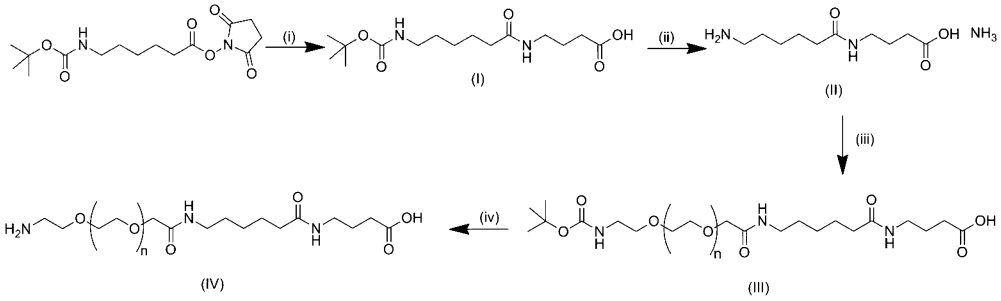

Figure 8. Synthetic route used to synthesize the GABA ligand. (i) Pyridine, GABA, ambient temperature, 18 h; (ii) TFA, methylene chloride, ambient temperature, 1 h; (iii) BOC-NH-PEG-NHS, methylene chloride, pyridine, ambient temperature, 48 h; (iv) TFA, methanol, ambient temperature, 2 h.

carbodiimide hydrochloride (EDC), Dowex 50WX4-50 exchange resin, and pyridine were obtained from Aldrich Chemical Corporation (Milwaukee, WI). Methylene chloride was obtained from Fisher BioReagents Scientific (Fair Lawn, NJ) and used without purification. Magnesium sulfate was obtained from VWR International (West Chester, PA). All NMR measurements were performed using a Bruker 300 MHz machine. Chemical shifts were measured relative to TMS.

Synthesis of Conjugates. Muscimol-conjugated quantum dots were synthesized using previously described protocols.[40,46] The GABA ligand used in these studies was composed of GABA attached to polydisperse PEG 3400 via a short (6-aminohexanoyl; AH) spacer. The other end of the PEG was terminated with an amino functionality, and this formed the point of attachment to the AMP coating on the qdot surface. The GABA ligand (IV) was synthesized as outlined in Figure 8. *N*-Hydroxysuccinimide ester (BOC-AH-NHS), synthesized as described by Doughty et al.,[52] was reacted with γ-aminobutyric acid (GABA) to yield (**I**) in a 44% yield. The BOC protecting group was subsequently removed with trifluoroacetic acid to give AH-GABA (**II**) in a 68% yield. This was coupled to BOC-NH-PEG-CONHS to give the BOC protected intermediate (BOC-NH-PEG-AH-GABA) (**III**), which was converted to the GABA ligand (NH_2-PEG-AH-GABA) (**IV**) by treatment with trifluoroacetic acid. MALDI-MS of the NH_2-PEG-AH-GABA was consistent with compound (**IV**).

4-(6-(tert-Butoxycarbonylamino)hexanamido)butanoic Acid (I). 6-*tert*-Butoxycarbonylaminohexanoic acid 2,5-dioxopyrrolidin-1-yl ester (4 g, 12.2 mmol) and γ-aminobutanoic acid (1.25 g, 12.2 mmol) were dissolved in dry pyridine (50 mL). The solution was stirred at ambient temperature for 18 h and then evaporated under reduced pressure. The resulting residue was washed with diethyl ether (1 × 100 mL) and then was dissolved in methylene chloride (100 mL). This was washed with hydrochloric acid (2M, 2 × 50 mL) and dried over anhydrous magnesium sulfate. The solution was filtered and evaporated to give 1.7 g (44%) of 4-(6-(*tert*-butoxycarbonylamino)-hexanamido)butanoic acid as a yellow oil. ^{1}H NMR ($CDCl_3$) 1.30−1.50 (m, 11H), 1.66 (t, 2H), 1.88 (t, 2H), 2.18 (m, 5H), 2.39 (t, 2H), 3.11 (q, 2H), 3.33 (q, 2H), 4.78 (s, 1H), 6.37 (s, 1H). ^{13}C NMR ($CDCl_3$) 24.11, 25.11, 26.04, 28.34, 29.65, 30.88, 31.76, 36.32, 39.27, 40.21, 173.78, 176.58.

4-(6-Aminohexanamido)butanoic Acid Ammonium Salt (II). 4-(6-(*tert*-Butoxycarbonylamino)hexanamido)butanoic acid (1.6 g, 5 mmol) was dissolved in methylene chloride (2 mL), and trifluoroacetic acid (2 mL) was added. The solution was stirred at ambient temperature for 1 h and then evaporated under reduced pressure. The resulting residue was dissolved in deionized water (2 mL); the product was purified on Dowex 50WX4-50 exchange resin that was initially eluted with deionized water and then eluted with amonium hydroxide solution. The fractions containing the 4-(6-aminohexanamido)-butanoic acid were visualized on silica TLC plates by staining with ninhydrin, and these were evaporated under reduced pressure to give 0.79 g (68%) of 4-(6-aminohexanamido)butanoic acid ammonium salt (**II**) as a white solid. ^{1}H NMR (D_2O) 1.21−1.31 (m, 2H), 1.47−1.66 (m, 6H), 1.95−2.14 (m, 4H), 2.87 (t, 2H), 3.08 (t, 2H), 4.69 (s, 7H). ^{13}C NMR (D_2O) 24.74, 24.98, 25.09, 26.38, 34.29, 35.42, 38.99, 39.22, 176.56, 181.95.

BOC-Protected GABA Derivative (III). An amount of 0.2 g of *tert*-butyloxycarbonyl (BOC) amine-PEG-activated acid (BOC-NH-PEGNHS) was weighed out in a round-bottomed flask, and methylene chloride (100 mL) was added. Then 0.016 g of 4-(6-aminohexanamido)butanoic acid ammonium salt (**II**) was dissolved in dry pyridine (2 mL), and this solution was added to the methylene chloride solution. The resulting mixture was stirred at ambient temperature for 48 h and then evaporated under reduced pressure. The crude product was washed with diethyl ether (6 × 100 mL) and dried under reduced pressure to yield 0.2 g of the BOC protected GABA derivative (**III**) as a white solid.

Deprotected GABA Derivative (IV). An amount of 0.16 g of the BOC protected GABA derivative (**III**) was dissolved in methanol (5 mL), and trifluoroacetic acid (3 mL) was added. This solution was stirred at ambient temperature for 2 h; the solution was then evaporated under reduced pressure. The final product was washed with diethyl ether (10 × 100 mL) and dried under reduced pressure to give 0.12 g of the GABA derivative (**IV**) as a white solid.

Ligand Coupling. NH_2-PEG-AH-GABA was conjugated to terminating carboxyl groups on the AMP coated qdots using 1-[3-(dimethylamino)propyl]-3-ethylcarbodiimide hydrochloride (EDC). A volume of 0.1 mL of an 8 μM solution of qdots was placed in a vial equipped with a stir bar. To this was added 0.3 mL of borate buffer (pH 8.5) that contained 3 mg (1000 equiv) of the GABA ligand (NH_2-PEG-AH-GABA) (**IV**). Then *N*-hydroxysuccinimide (72 μg, 0.63 μmol) dissolved in borate buffer (0.1 mL) was added. This was followed by the addition of 1-[3-(dimethylamino)propyl]-3-ethyl-carbodiimide hydrochloride (EDC) (0.12 mg, 0.63 μmol) dissolved in borate buffer (0.1 mL). The mixture was stirred at room temperature for 2 h, then purified by passage through a Sephadex G-50 column, and eluted with borate buffer (pH 8.5). The fluorescent fractions were combined to yield the purified GABA-functionalized qdots (GABA-PEG-qdots). The concentration of the resulting GABA-conjugated qdots was determined to be 580 nM using UV−visible spectroscopy, based on measurement of the absorption feature at 600 nm and use of 6.5×10^5 M^{-1} cm^{-1} as extinction coefficient. The GABA-conjugated qdots were characterized using agarose gel electrophoresis.

Ligand loading of the qdot was governed by the number of molar equivalents (relative to that of the qdot) of added ligand and EDC[31,46] as well as by steric constraints and the availability of free carboxylic groups on the AMP-coated qdot surface. With muscimol-terminated ligand, use of a large excess of ligand (2000 equivalents) led to precipitation of the conjugate,[40] perhaps due to ligand cross-linking through electrostatic or hydrogen bonding interactions or to general insolubility. Quantum dots with an excessively high loading of ligand might be deleterious for studies aimed at the tracking of single GABA receptors, particularly if the receptors were expressed at high density on the cell surface.

Oocyte Preparation. All animal procedures adhered to institutional policies and to the Statement for the Use of Animals in Ophthalmic and Vision Research adopted by the Association for

Research in Vision and Ophthalmology (ARVO). Oocytes were obtained from *Xenopus laevis* toads (*Xenopus* One, Ann Arbor, MI), and $\alpha1\beta2\gamma2$ $GABA_A$ (rat $\alpha1$, rat $\beta2$, human $\gamma2$ subunits) or homopentameric human $\rho1$ $GABA_A$ receptors were expressed in the oocytes through injection of RNA synthesized in vitro (mMessage mMachine, Ambion/Applied Biosystems by Life Technologies, Austin, TX) as previously described.[9,18] Oocytes that were not injected with RNA, that is, did not express the $GABA_A$ receptors, were used as controls.

Quantitative Fluorescence Microscopy. Visualization and quantification procedures relevant to the fluorescence analysis of oocytes expressing $\alpha1\beta2\gamma2$ $GABA_A$ receptors or $\rho1$ $GABA_A$ receptors, and (control) nonexpressing (NE) oocytes followed methods similar to those previously described.[40,46] Specifically, fluorescence and bright-field images were obtained from oocytes positioned in glass-bottom dishes (MatTek Corp., Ashland, MA) and incubated for defined periods in physiological solution supplemented with the test components. Fluorescence was measured using a confocal microscope (Leica model DM-IRE2 with 20× objective; λ excitation = 476 nm; λ emission = 580−620 nm; peak emission λ = 600−605 nm). Microscope settings relevant to excitation illumination and detection of fluorescence emission were established at the beginning of each series of experiments and remained unchanged for the entire group of measurements. Experiments on a given day were performed on a single batch of oocytes and employed a single preparation of test solutions. Each fluorescence image was quantified (0−255 scale) using MetaMorph version 7.0r4 software (Universal Imaging Corp., Downingtown, PA), as previously described.[40,46] Briefly, the arclike border of the oocyte was traced and it included 500−725 pixels (i.e., data points). For determination of background fluorescence (fluorescence of the medium bathing the oocyte), the line used to determine the border fluorescence was replicated to cover a representative region in the medium. For each image, the fluorescence intensities in the pixels along the two segmented lines (at the oocyte border and background) were then obtained. Net fluorescence intensity (FI) in each image was defined as the difference in the mean fluorescence intensity in the two lines, each consisting of a total of I pixels:

$$\mathrm{FI} = \left(\sum_{i=1}^{I} \mathrm{BDFI}_i\right)/I - \left(\sum_{i=1}^{I} \mathrm{BGFI}_i\right)/I \quad (1)$$

where BDFI_i and BGFI_i are fluorescence intensities of the ith pixel in the oocyte border and background, respectively.

Statistical Methods. The segmented lines representing the oocyte border and background within each image consisted of ∼500−725 data points, or equivalently, each image corresponded with 1000−1450 data points. Because of the large number of data points representing each image, we determined the net fluorescence intensity FI for each image and then used a t test to compare the FI obtained for a given pair of experimental conditions. Because this approach (i.e., single data point per image) is highly conservative in terms of statistical power, compared with an alternative approach that compares conditions using a hierarchical method for all of the pixel values in each image (1000−1450 data points per image), we further decided not to correct the determined p-values for multiple comparisons. Any p-value < 0.05 resulting from a one-sided t test was considered to be statistically significant.

AUTHOR INFORMATION

Corresponding Author

*Mailing address: Dept. of Ophthalmology and Visual Sciences, University of Illinois at Chicago, 1855 W. Taylor St., Chicago, IL 60612. Telephone: 312-996-4262. Fax: 312-996-7773. E-mail: davipepp@uic.edu.

Author Contributions

I.D.T. carried out the synthesis, purification, and chemical characterization of GABA-qdot and muscimol-qdot conjugates. H.A.G. conducted the oocyte binding experiments and fluorescence analyses. D.C. performed the statistical analyses. S.J.R. and D.R.P. directed, respectively, the chemical syntheses and pharmacological experiments. H.A.G., I.D.T., H.Q., S.J.R., and D.R.P. conceived the project. All authors contributed to writing of the paper.

Funding

This work was supported by NIH grants EY016094, EY001792, EB003728, and EM72048; by grants from the Daniel F. and Ada L. Rice Foundation (Skokie, IL); by the Macular Degeneration Research Program of the American Health Assistance Foundation (Clarksburg, MD); by Hope for Vision (Washington, DC), by Research to Prevent Blindness (New York, NY); by the Beckman Initiative for Macular Research (Los Angeles, CA); by award UL1RR029879 from the University of Illinois at Chicago Center for Clinical and Translational Science (CCTS); by the Cless Family Foundation (Northbrook, IL); and by the Intramural Program of the National Eye Institute.

Notes

The authors declare no competing financial interest.

ACKNOWLEDGMENTS

We thank Ms. Feng Feng and Ms. Ruth Zelkha for technical assistance and Dr. Deborah M. Little for helpful discussions.

REFERENCES

(1) Macdonald, R. L., and Olsen, R. W. (1994) $GABA_A$ receptor channels. *Annu. Rev. Neurosci. 17*, 569−602.

(2) Sieghart, W., and Sperk, G. (2002) Subunit composition, distribution and function of $GABA_A$ receptor subtypes. *Curr. Top. Med. Chem. 2*, 795−816.

(3) Olsen, R. W., and Sieghart, W. (2008) International Union of Pharmacology. LXX. Subtypes of γ-aminobutyric $acid_A$ receptors: classification on the basis of subunit composition, pharmacology, and function. Update. *Pharmacol. Rev. 60*, 243−260.

(4) Olsen, R. W., and Sieghart, W. (2009) $GABA_A$ receptors: Subtypes provide diversity of function and pharmacology. *Neuropharmacology 56*, 141−148.

(5) Cutting, G. R., Lu, L., O'Hara, B. F., Kasch, L. M., Montrose-Rafizadeh, C., Donovan, D. M., Shimada, S., Antonarakis, S. E., Guggino, W. B., Uhl, G. R., and Kazazian, H. H., Jr. (1991) Cloning of the γ-aminobutyric acid (GABA) $\rho1$ cDNA: a GABA receptor subunit highly expressed in the retina. *Proc. Natl. Acad. Sci. U.S.A. 88*, 2673−2677.

(6) Polenzani, L., Woodward, R. M., and Miledi, R. (1991) Expression of mammalian γ-aminobutyric acid receptors with distinct pharmacology in *Xenopus* oocytes. *Proc. Natl. Acad. Sci. U.S.A. 88*, 4318−4322.

(7) Drew, C. A., and Johnston, G. A. (1992) Bicuculline- and baclofen-insensitive gamma-aminobutyric acid binding to rat cerebellar membranes. *J. Neurochem. 58*, 1087−1092.

(8) Qian, H., Hyatt, G., Schanzer, A., Hazra, R., Hackam, A. .S, Cutting, G. R., and Dowling, J. E. (1997) A comparison of $GABA_C$ and ρ subunit receptors from the white perch retina. *Visual Neurosci. 14*, 843−851.

(9) Qian, H., Dowling, J. E., and Ripps, H. (1998) Molecular and pharmacological properties of GABA-ρ subunits from white perch retina. *J. Neurobiol. 37*, 305−320.

(10) Kumar, R. J., Chebib, M., Hibbs, D. E., Kim, H. L., Johnston, G. A., Salam, N. K., and Hanrahan, J. R. (2008) Novel γ-aminobutyric acid $\rho1$ receptor antagonists; synthesis, pharmacological activity and structure−activity relationships. *J. Med. Chem. 51*, 3825−3840.

(11) Chebib, M. (2004) $GABA_C$ receptor ion channels. *Clin. Exp. Pharmacol. Physiol. 31*, 800−804.

(12) Martínez-Delgado, G., Estrada-Mondragón, A., Miledi, R., and Martínez-Torres, A. (2010) An update on GABAρ receptors. *Curr. Neuropharmacol. 8*, 422−433.
(13) Feigenspan, A., and Bormann, J. (1994) Differential pharmacology of $GABA_A$ and $GABA_C$ receptors on rat retinal bipolar cells. *Eur. J. Pharmacol. 288*, 97−104.
(14) Murata, Y., Woodward, R. M., Miledi, R., and Overman, L. E. (1996) The first selective antagonist for a $GABA_C$ receptor. *Bioorg. Med. Chem. Lett. 6*, 2073−2076.
(15) Ragozzino, D., Woodward, R. M., Murata, Y., Eusebi, F., Overman, L. E., and Miledi, R. (1996) Design and *in vitro* pharmacology of a selective γ-aminobutyric $acid_C$ antagonist. *Mol. Pharmacol. 50*, 1024−1030.
(16) Chebib, M., Hanrahan, J. R., Kumar, R. J, Mewett, K. N., Morriss, G., Wooller, S., and Johnston, G. A. (2007) (3-Aminocyclopentyl)methylphosphinic acids: novel $GABA_C$ receptor antagonists. *Neuropharmacology 52*, 779−787.
(17) Xie, A., Yan, J., Yue, L., Feng, F., Mir, F., Abdel-Halim, H., Chebib, M., Le Breton, G. C., Standaert, R. F., Qian, H., and Pepperberg, D. R. (2011) 2-Aminoethyl methylphosphonate, a potent and rapidly acting antagonist of $GABA_A$-ρ1 receptors. *Mol. Pharmacol. 80*, 965−978.
(18) Vu, T. Q., Chowdhury, S., Muni, N. J., Qian, H., Standaert, R. F., and Pepperberg, D. R. (2005) Activation of membrane receptors by a neurotransmitter conjugate designed for surface attachment. *Biomaterials 26*, 1895−1903.
(19) McBride, J., Treadway, J., Feldman, L. C., Pennycook, S. J., and Rosenthal, S. J. (2006) Structural basis for near unity quantum yield core/shell nanostructures. *Nano Lett. 6*, 1496−1501.
(20) Medintz, I. L., Uyeda, H. T., Goldman, E. R., and Mattoussi, H. (2005) Quantum dot bioconjugates for imaging, labelling and sensing. *Nat. Mater. 4*, 435−446.
(21) Jaiswal, J. K., and Simon, S. M. (2007) Imaging single events at the cell membrane. *Nat. Chem. Biol. 3*, 92−98.
(22) Willner, I., Basnar, B., and Willner, B. (2007) Nanoparticle-enzyme hybrid systems for nanobiotechnology. *FEBS J. 274*, 302−309.
(23) Biju, V., Itoh, T., Anas, A., Sujith, A., and Ishikawa, M. (2008) Semiconductor quantum dots and metal nanoparticles: syntheses, optical properties, and biological applications. *Anal. Bioanal. Chem. 391*, 2469−2495.
(24) Rosenthal, S. J., Tomlinson, I., Adkins, E. M., Schroeter, S., Adams, S., Swafford, L., McBride, J., Wang, Y., DeFelice, L. J., and Blakely, R. D. (2002) Targeting cell surface receptors with ligand-conjugated nanocrystals. *J. Am. Chem. Soc. 124*, 4586−4594.
(25) Tomlinson, I. D., Gies, A. P., Gresch, P. J., Dillard, J., Orndorff, R. L., Sanders-Bush, E., Hercules, D. M., and Rosenthal, S. J. (2006) Universal polyethylene glycol linkers for attaching receptor ligands to quantum dots. *Bioorg. Med. Chem. Lett. 16*, 6262−6266.
(26) Tomlinson, I. D., Iwamoto, H., Blakely, R. D., and Rosenthal, S. J. (2011) Biotin tethered homotryptamine derivatives: High affinity probes of the human serotonin transporter (SERT). *Bioorg. Med. Chem. Lett. 21*, 1678−1682.
(27) Bruchez, M., Jr., Moronne, M., Gin, P., Weiss, S., and Alivisatos, A. P. (1998) Semiconductor nanocrystals as fluorescent biological labels. *Science 281*, 2013−2016.
(28) Mattoussi, H., Mauro, J. M., Goldman, E. R., Anderson, G. P., Sundar, V. C., Mikulec, F. V., and Bawendi, M. G. (2000) Self-assembly of CdSe-ZnS quantum dot bioconjugates using an engineered recombinant protein. *J. Am. Chem. Soc. 122*, 12142−12150.
(29) Dahan, M., Lévi, S., Luccardini, C., Rostaing, P., Riveau, B., and Triller, A. (2003) Diffusion dynamics of glycine receptors revealed by single-quantum dot tracking. *Science 302*, 442−445.
(30) Goldman, E. R., Clapp, A. R., Anderson, G. P., Uyeda, H. T., Mauro, J. M., Medintz, I. L., and Mattoussi, H. (2004) Multiplexed toxin analysis using four colors of quantum dot fluororeagents. *Anal. Chem. 76*, 684−688.
(31) Bentzen, E. L., Tomlinson, I. D., Mason, J., Gresch, P., Warnement, M. R., Wright, D., Sanders-Bush, E., Blakely, R., and Rosenthal, S. J. (2005) Surface modification to reduce nonspecific binding of quantum dots in live cell assays. *Bioconjugate Chem. 16*, 1488−1494.
(32) Mason, J. N., Farmer, H., Tomlinson, I. D., Schwartz, J. W., Savchenko, V., DeFelice, L. J., Rosenthal, S. J., and Blakely, R. D. (2005) Novel fluorescence-based approaches for the study of biogenic amine transporter localization, activity, and regulation. *J. Neurosci. Methods 143*, 3−25.
(33) Robinson, A., Fang, J. M., Chou, P. T., Liao, K. W., Chu, R. M., and Lee, S. J. (2005) Probing lectin and sperm with carbohydrate-modified quantum dots. *ChemBioChem 6*, 1899−1905.
(34) Tomlinson, I. D., Mason, J. N., Blakely, R. D., and Rosenthal, S. J. (2005) Peptide-conjugated quantum-dots: imaging the angiotensin type 1 receptor in living cells. *Methods Mol. Biol. 303*, 51−60.
(35) Anikeeva, N., Lebedeva, T., Clapp, A. R., Goldman, E. R., Dustin, M. L., Mattoussi, H., and Sykulev, Y. (2006) Quantum dot/peptide-MHC biosensors reveal strong CD8-dependent cooperation between self and viral antigens that augment the T cell response. *Proc. Natl. Acad. Sci. U.S.A. 103*, 16846−16851.
(36) Pathak, S., Davidson, M. C., and Silva, G. A. (2007) Characterization of the functional binding properties of antibody conjugated quantum dots. *Nano Lett. 7*, 1839−1845.
(37) Orndorff, R. L., Warnement, M. R., Mason, J. N., Blakely, R. D., and Rosenthal, S. J. (2008) Quantum dot *ex vivo* labeling of neuromuscular synapses. *Nano Lett. 8*, 780−785.
(38) Rajan, S. S., Liu, H. Y., and Vu, T. Q. (2008) Ligand-bound quantum dot probes for studying the molecular scale dynamics of receptor endocytic trafficking in live cells. *ACS Nano 2*, 1153−1166.
(39) Kovtun, O., Tomlinson, I. D., Sakrikar, D. S., Chang, J. C., Blakely, R. D., and Rosenthal, S. J. (2011) Visualization of the cocaine-sensitive dopamine transporter with ligand conjugated quantum dots. *ACS Chem. Neurosci. 2*, 370−378.
(40) Gussin, H. A., Tomlinson, I. D., Little, D. M., Warnement, M. R., Qian, H., Rosenthal, S. J., and Pepperberg, D. R. (2006) Binding of muscimol-conjugated quantum dots to $GABA_C$ receptors. *J. Am. Chem. Soc. 128*, 15701−15713.
(41) Tomlinson, I. D., Gussin, H. A., Little, D. M., Warnement, M. R., Qian, H., Pepperberg, D. R, and Rosenthal, S. J. (2007) Imaging $GABA_C$ receptors with ligand-conjugated quantum dots. *J. Biomed. Biotechnol. 2007*, 76514.
(42) Enz, R., and Cutting, G. R. (1998) Molecular composition of $GABA_C$ receptors. *Vision Res. 38*, 1431−1441.
(43) Qian, H., Dowling, J. E., and Ripps, H. (1999) A single amino acid in the second transmembrane domain of GABA ρ subunits is a determinant of the response kinetics of $GABA_C$ receptors. *J. Neurobiol. 10*, 67−76.
(44) Sedelnikova, A., Smith, C. D., Zakharkin, S. O., Davis, D., Weiss, D. S., and Chang, Y. (2005) Mapping the ρ1 $GABA_C$ receptor agonist binding pocket: constructing a complete model. *J. Biol. Chem. 280*, 1535−1542.
(45) Yamamoto, I., Carland, J. E., Locock, K., Gavande, N., Absalom, N., Hanrahan, J. R., Allan, R., D., Johnston, G. A. R., and Chebib, M. (2012) Structurally diverse GABA antagonists interact differently with open and closed conformational states of the ρ1 receptor. *ACS Chem. Neurosci. 3*, 293−301.
(46) Gussin, H. A., Tomlinson, I. D., Muni, N. J., Little, D. M., Qian, H., Rosenthal, S. J., and Pepperberg, D. R. (2010) $GABA_C$ receptor binding of quantum-dot conjugates of variable ligand valency. *Bioconjugate Chem. 21*, 1455−1464.
(47) Gussin, H. A., Tomlinson, I. D., Little, D. M., Qian, H., Rosenthal, S. J., and Pepperberg, D. R. (2009) Quantum dot conjugates of GABA and muscimol: binding to $GABA_A$ and $GABA_C$ receptors. Program No. 114.4, 2009 Annual Meeting of the Society for Neuroscience, Chicago, IL, Society for Neuroscience, Online.
(48) Chebib, M., and Johnston, G. A. R. (2000) GABA-activated ligand gated ion channels: medicinal chemistry and molecular biology. *J. Med. Chem. 43*, 1427−1447.
(49) Krogsgaard-Larsen, P., Frølund, B., and Ebert, B. (1997) $GABA_A$ receptor agonists, partial agonists, and antagonists. In *The GABA*

receptors (Enna, S. J., and Bowery, N. G., Eds.), pp 31−81, Humana Press, Totowa, NJ.
(50) Johnston, G. A. R. (1996) $GABA_C$ receptors: relatively simple transmitter-gated ion channels? *Trends Pharmacol. Sci. 17*, 319−323.
(51) Bouzigues, C., Lévi, S., Triller, A., and Dahan, M. (2007) Single quantum dot tracking of membrane receptors. *Methods Mol. Biol. 374*, 81−91.
(52) Doughty, M. B., Chaurasia, C. S., and Li, K. (1993) Benextramine-neuropeptide Y receptor interactions: contribution of the benzylic moieties to $^{[3H]}$neuropeptide Y displacement activity. *J. Med. Chem. 36*, 272−279.